First-principles study on the origin of low charging overpotential of the sodium oxygen batteries

Byungju Lee[1], Dong-Hwa Seo[2], Hee-Dae Lim[1], Inchul Park[1], Kyu-Young Park[1], Jinsoo Kim[1], and Kisuk Kang[2,*]

[1]Department of Materials Science and Engineering, Seoul National University, Seoul, 151-742, Republic of Korea

[2]Department of Materials Science and Engineering, Research Institute of Advanced Materials, Seoul National University, Seoul, 151-742, Republic of Korea

Supplementary Material

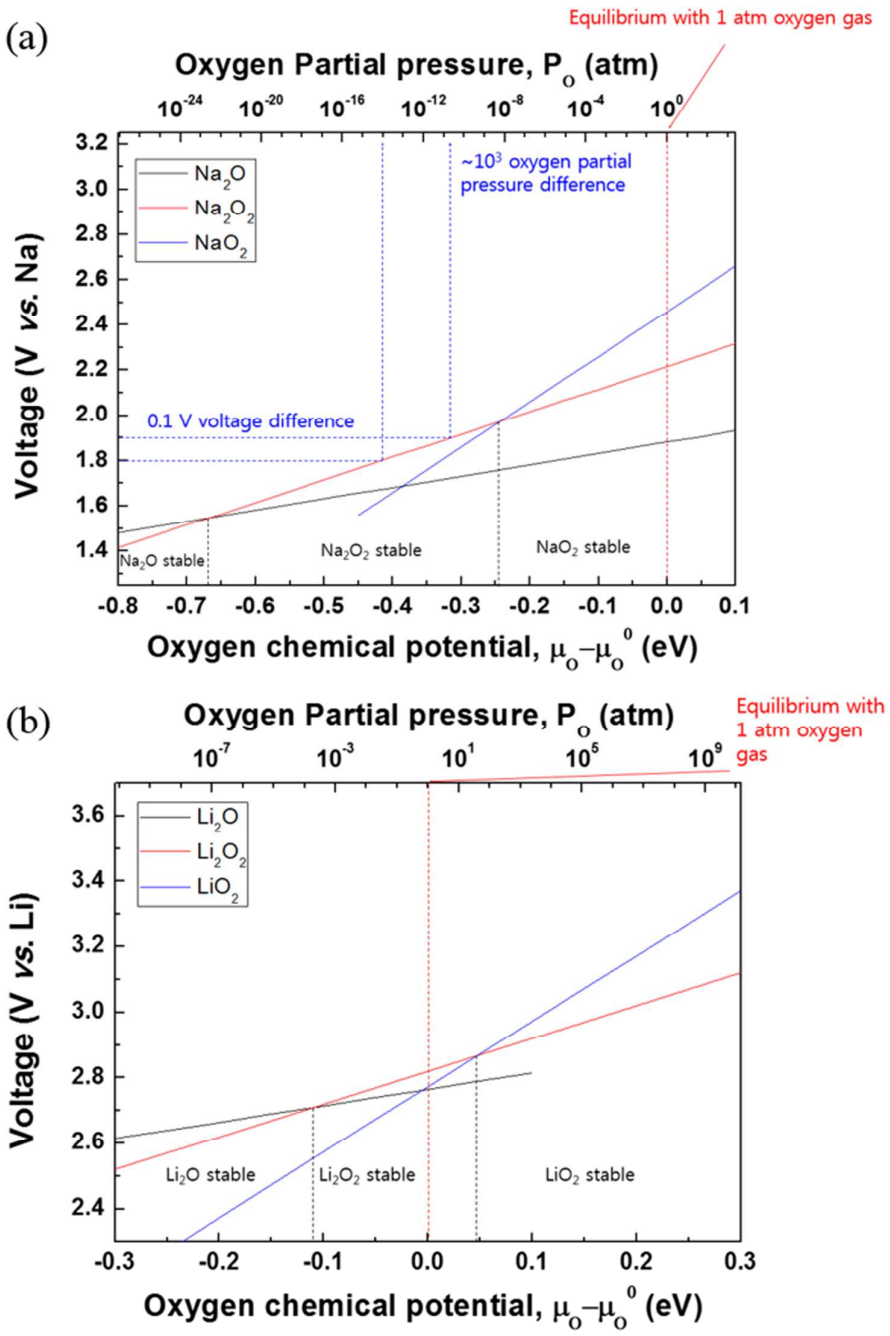

Figure S1. Relationship between cell voltage and oxygen partial pressure, (a) in the Na/O_2 cell and (b) in the Li/O_2 cell. Higher cell voltage is related with more negative Gibbs free energy, according to Nernst equation; $\mu_{metal} - \mu_{metal}{}^0 = -nFE_{cell}$, where μ_{metal} is chemical potential of metal (Na or Li) in structure, $\mu_{metal}{}^0$ is chemical potential of pure metal, n is the number of charge of metal ion, F is faraday constant, E_{cell} is the voltage of the cell.

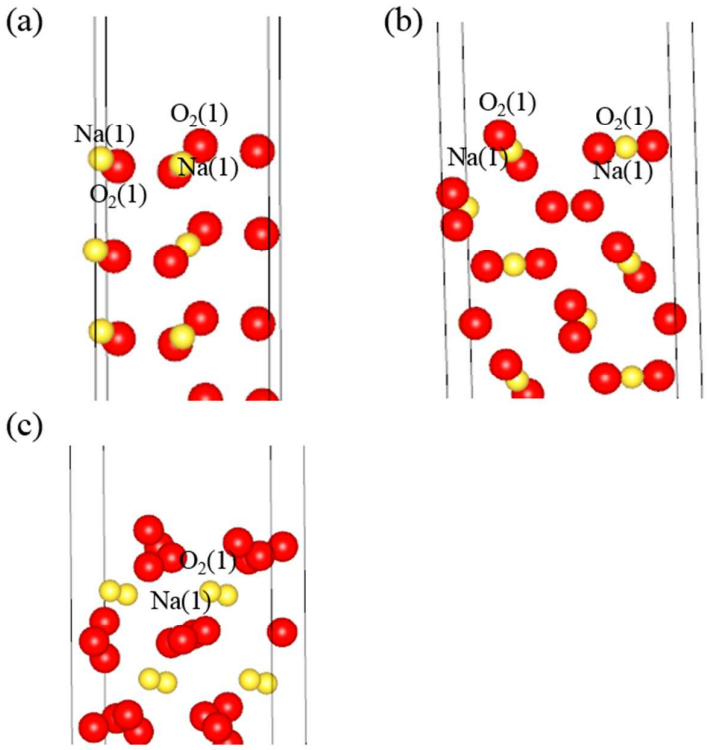

Figure S2. Surface unit cells of pyrite NaO_2. The yellow and red atoms correspond to sodium and oxygen, respectively. Three low-index surfaces were considered. As termination with an O atom rather than an O_2 dumbbell made the surface unstable, such terminations were not considered in this study.

Orientation	Termination	Na_2O_2 limit	O_2 limit
(100)	O_2(1)-Na(1)*	13	13
	O_2(1)	48	21
	Na(1)	128	156
(110)	O_2(1)-Na(1)-Na(2)*	26	26
	O_2(1)	62	42
	Na(1)-Na(2)	51	70
	O_2(1)-Na(1)	28	18
(111)	O_2(1)	34	18
	Na(1)	42	58

Table S1. Surface energies of pyrite NaO_2 for all possible terminations. The star symbols (*) indicate stoichiometric surfaces. The most stable termination of each surface was used to construct the Wulff shape. (in meV/Å^2)

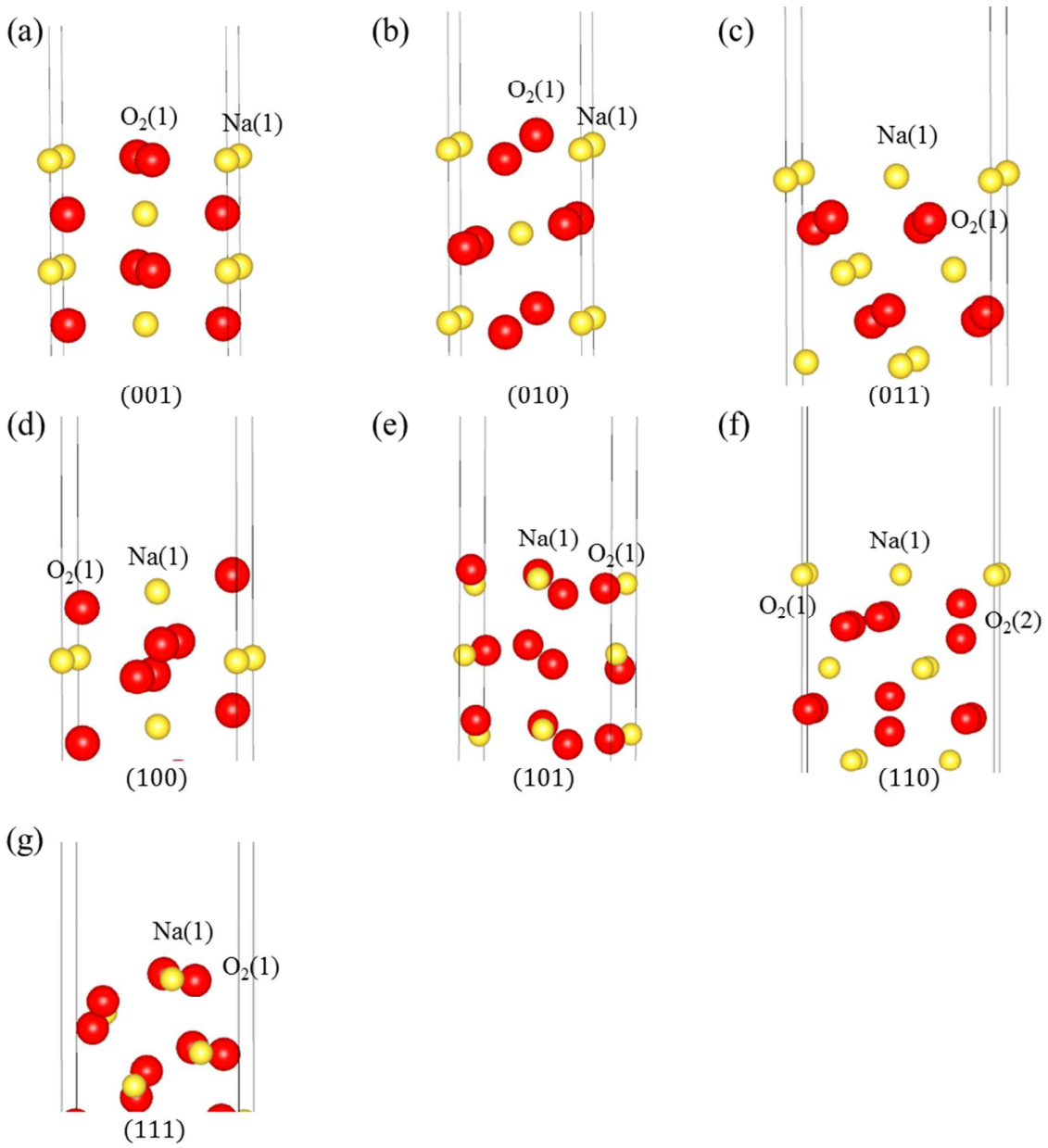

Figure S3. Surface unit cells of marcasite NaO_2. The yellow and red atoms correspond to sodium and oxygen, respectively. Seven low-index surfaces were considered.

Orientation	Termination	Na_2O_2 limit	O_2 limit
(001)	O_2(1)-Na(1)*	29	29
	O_2(1)	35	15
	Na(1)	68	89
(010)	O_2(1)-Na(1)*	23	23
	O_2(1)	52	18
	Na(1)	140	174
(011)	O_2(1)-Na(1)	57	75
	O_2(1)	32	14
(100)	O_2(1)-Na(1)*	37	37
	O_2(1)	49	24
	Na(1)	90	116
(101)	O_2(1)-Na(1)*	16	16
	O_2(1)	47	15
	Na(1)	76	92
(110)	Na(1)-O_2(1)-O_2(2)	65	85
	O_2(1)-O_2(2)	42	21
	O_2(1)*	37	37
	O_2(2)*	37	37
(111)	O_2(1)-Na(1)*	25	25
	O_2(1)	32	17
	Na(1)	52	66

Table S2. Surface energies of NaO_2 for all possible terminations. The star symbols (*) indicate stoichiometric surfaces. (in meV/Å^2)

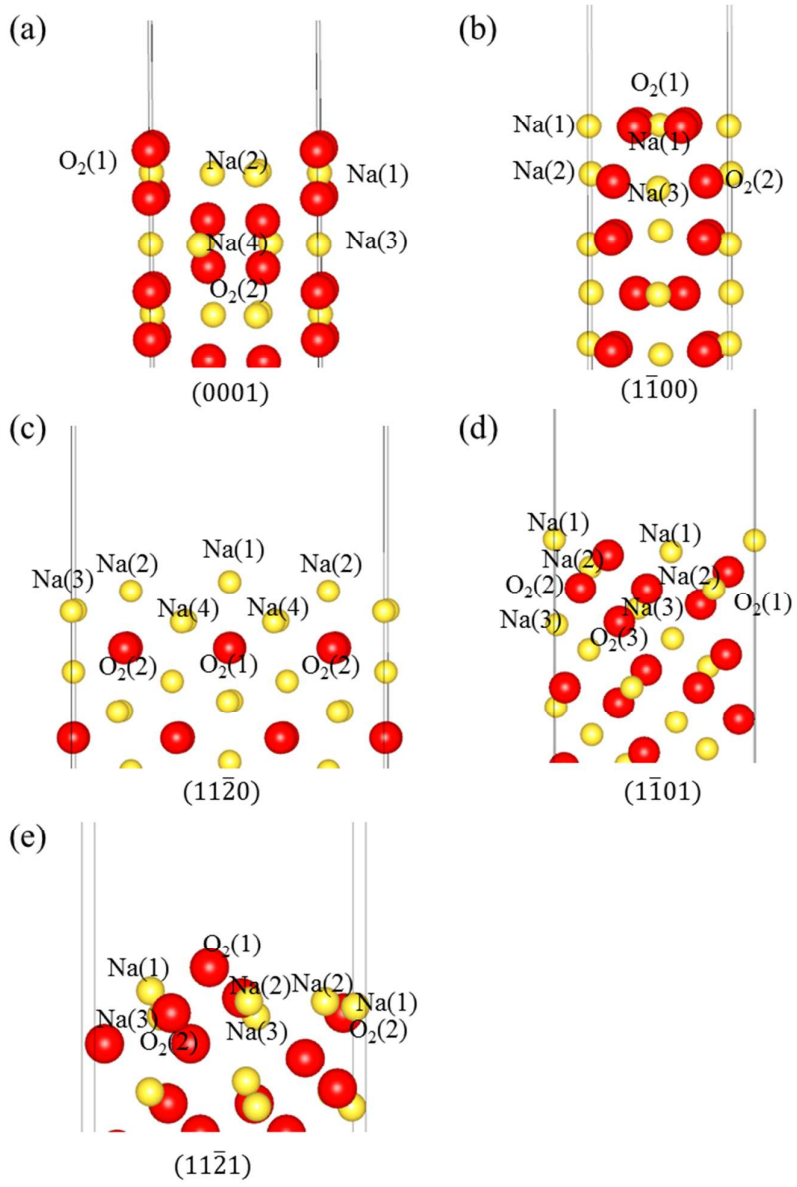

Figure S4. Surface unit cells of Na_2O_2. The yellow and red atoms correspond to sodium and oxygen, respectively. Five low-index surfaces were considered. There were many terminations because of the low symmetry of the Na_2O_2 structure. The top and bottom surfaces of the $(11\bar{2}0)$ and $(11\bar{2}1)$ surfaces could not be terminated equally because of low symmetry, hence atoms that were positioned at the same crystallographic site were terminated.

Orientation	Termination	Na_2O limit	NaO_2 limit
(0001)	O_2(1)-Na(1)-Na(2)-O_2(2)-Na(3)-Na(4)	56	62
	Na(1)-Na(2)-O_2(2)-Na(3)-Na(4)	150	182
	O_2(1)-Na(2)-O_2(2)-Na(3)-Na(4)	43	37
	O_2(1)-Na(1)-O_2(2)-Na(3)-Na(4)	48	29
	O_2(1) -O_2(2)-Na(3)-Na(4)	73	41
	Na(1) -O_2(2)-Na(3)-Na(4)	69	76
	Na(2)-O_2(2)-Na(3)-Na(4)	36	55
	O_2(2)-Na(3)-Na(4)	35	28
	O_2(2)-Na(4)	54	34
	O_2(2)-Na(3)	66	34
	O_2(2)	84	39
$(1\bar{1}00)$	O_2(1)-Na(1)-Na(2)-O_2(2)-Na(3)*	47	47
	Na(1)-Na(2)-O_2(2)-Na(3)	149	180
	O_2(1) -Na(2)-O_2(2)-Na(3)	62	32
	Na(2)-O_2(2)-Na(3)*	51	51
	Na(2)-O_2(2)	49	34
	O_2(2)-Na(3)	50	35
	O_2(2)	63	32
	Na(2)	102	117
$(11\bar{2}0)$	Na(1)-Na(2)-Na(3)-Na(4)-O_2(1)-O_2(2)	136	162
	Na(2)-Na(3)-Na(4)-O_2(1)-O_2(2)	103	120
	Na(3)-Na(4)-O_2(1)-O_2(2)*	32	32
	Na(4)-O_2(1)-O_2(2)	40	31
	O_2(1)-O_2(2)	62	35
	O_2(1)	102	111
	O_2(2)	79	70
$(1\bar{1}01)$	Na(1)-O_2(1)-Na(2)-O_2(2)-Na(3)-O_2(3)	52	57
	O_2(1)-Na(2)-O_2(2)-Na(3)-O_2(3)	41	26
	Na(2)-O_2(2)-Na(3)-O_2(3)	77	82
	O_2(1)-O_2(2)-Na(3)-O_2(3)	73	38
	O_2(1)-Na(2) -Na(3)-O_2(3)	65	70
	O_2(1)-Na(3)-O_2(3)	56	41
	Na(2)-Na(3)-O_2(3)	125	150
	O_2(2)-Na(3)-O_2(3)	75	60
	Na(3)-O_2(3)	77	82
	Na(3)	124	148
	O_2(3)	54	49
$(11\bar{2}1)$	Na(1)-O_2(1)-Na(2)-O_2(2)-Na(3)*	45	45
	O_2(1)-Na(2)-O_2(2)-Na(3)	56	41
	Na(2)-O_2(2)-Na(3)*	76	76
	Na(2)-Na(3)	148	177
	Na(3)	98	112
	O_2(2)-Na(3)	60	46
	O_2(2)	203	174

Table S3. Surface energies of Na_2O_2 for all possible terminations. The star symbols (*) indicate stoichiometric surfaces. (in meV/Å^2)

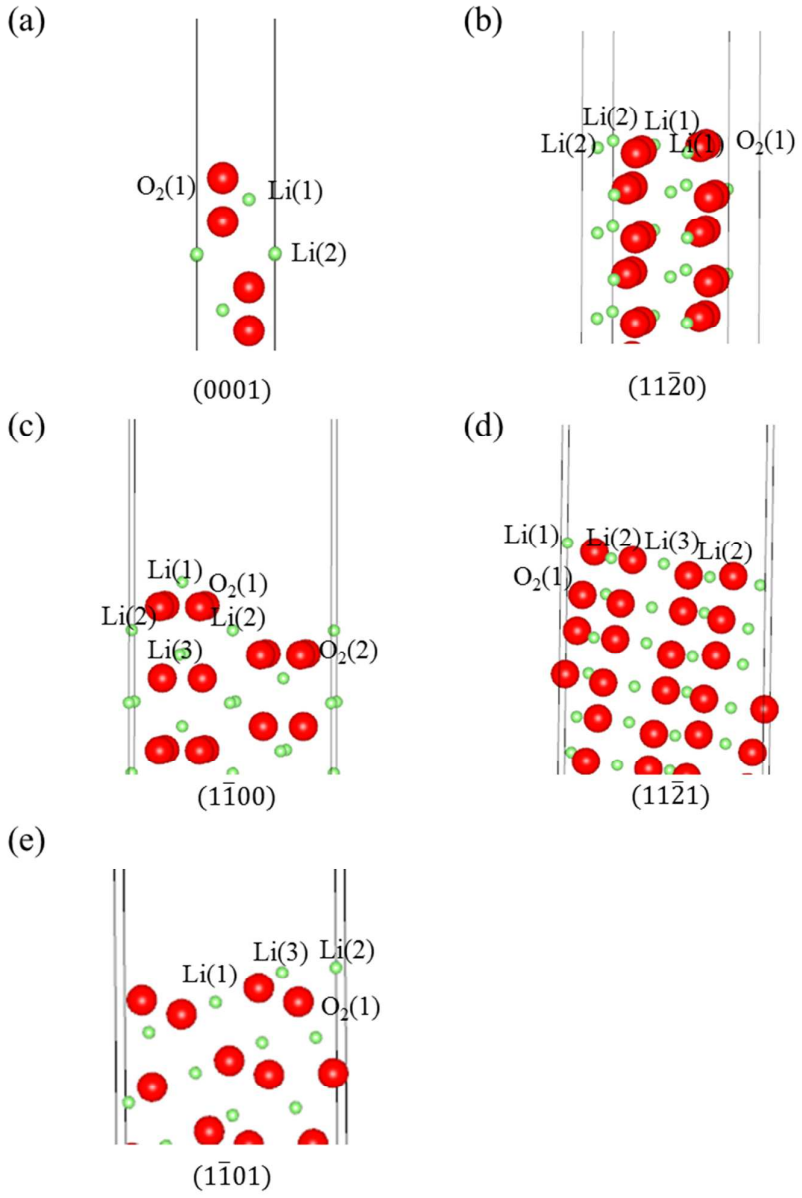

Figure S5. Surface unit cells of Li_2O_2. The green and red atoms correspond to lithium and oxygen, respectively. Five low-index surfaces were considered.

Orientation	Termination	Li_2O limit	O_2 limit
(0001)	O(1)-Li(1)-O(2)-Li(2)	38	32
	Li(1)-O(2)-Li(2)	65	72
	Li(2)	131	138
	O(2)-Li(2)	224	218
$(1\bar{1}00)$	Li(1)-O_2(2)-Li(3)*	35	35
	Li(1)-O_2(1)-Li(2)-O_2(2)-Li(3)	49	45
	O_2(1)-Li(2)-O_2(2)-Li(3)	68	60
	Li(2)-O_2(2)-Li(3)*	119	119
	O_2(2)-Li(3)	42	38
	Li(3)	131	136
$(11\bar{2}0)$	Li(1)-Li(2)-O_2(1)*	55	55
	Li(2)-O_2(1)	47	42
	Li(1)-O_2(1)	49	44
	O_2(1)	52	42
$(1\bar{1}01)$	Li(1)-Li(2)-Li(3)-O_2(1)	78	76
	Li(1)-Li(2)-O_2(1)	84	78
	Li(1)-Li(3)-O_2(1)	91	84
	Li(2)-Li(3)-O_2(1)	102	92
	Li(1)-O_2(1)	93	78
	Li(2)-O_2(1)	107	92
	Li(3)-O_2(1)	95	84
	O_2(1)	94	74
$(11\bar{2}1)$	Li(1)-Li(2)-Li(3)-O_2(1)	56	55
	Li(2)-Li(3)-O_2(1)	48	41
	Li(1)-Li(3)-O_2(1)	54	48
	Li(3)-O_2(1)	56	44

Table S4. Surface energies of Li_2O_2 for all possible terminations. The star symbols (*) indicate stoichiometric surfaces. (in meV/Å^2) The energies of terminations were in good agreement with the results of Mo *et al.*; [Reference 13 in the paper] slight differences derive from computational details. Note that Mo *et al.* referred to the $(11\bar{2}0)$ surface as $(1\bar{1}00)$, $(1\bar{1}00)$ as $(11\bar{2}0)$, $(11\bar{2}1)$ as $(1\bar{1}01)$, and $(1\bar{1}01)$ as $(11\bar{2}1)$. There are no stoichiometric terminations in the $(1\bar{1}01)$ and $(11\bar{2}1)$ surfaces, but Mo *et al.* considered stoichiometric terminations, resulting in different surface energies, for the $(1\bar{1}01)$ and $(11\bar{2}1)$ surfaces.

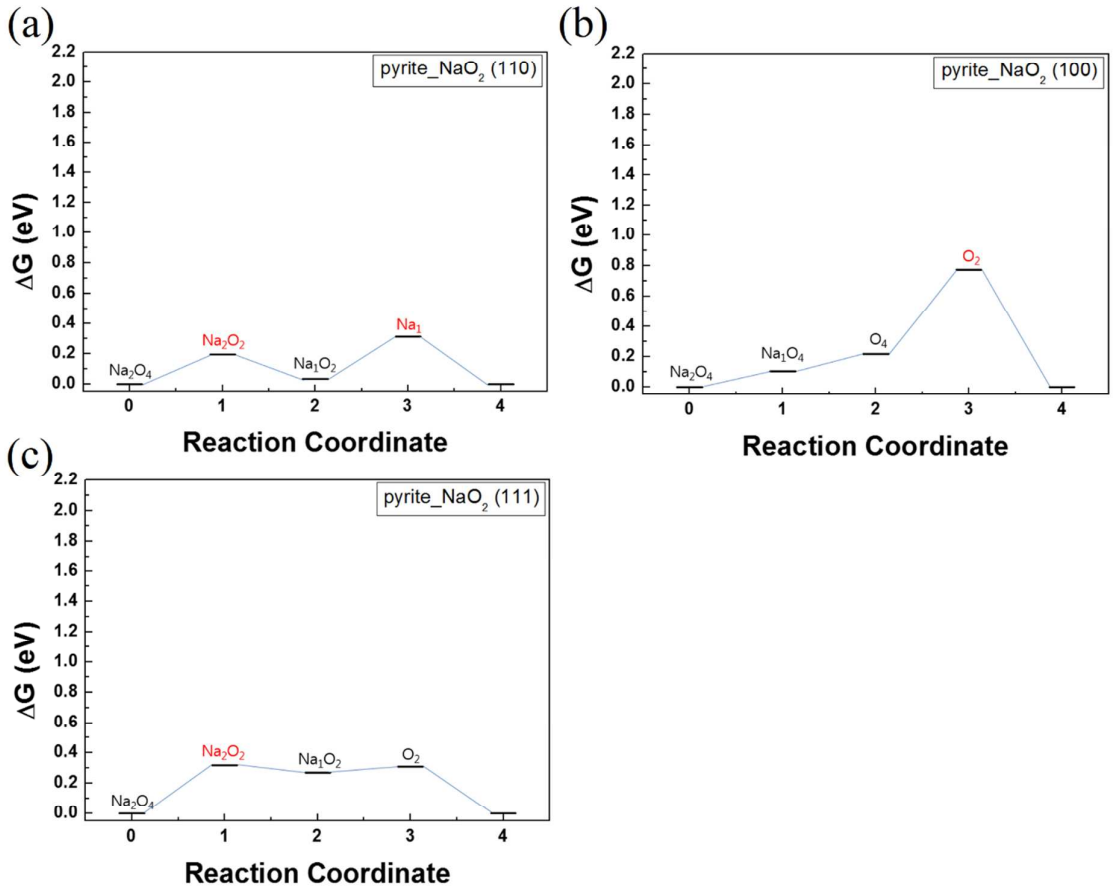

Figure S6. The OER energy profile for pyrite NaO_2. (a) (100) surface of pyrite NaO_2, (b) (110) surface of pyrite NaO_2, (c) (111) surface of pyrite NaO_2. The most favorable reaction paths are shown. The chemical steps are shown in red.

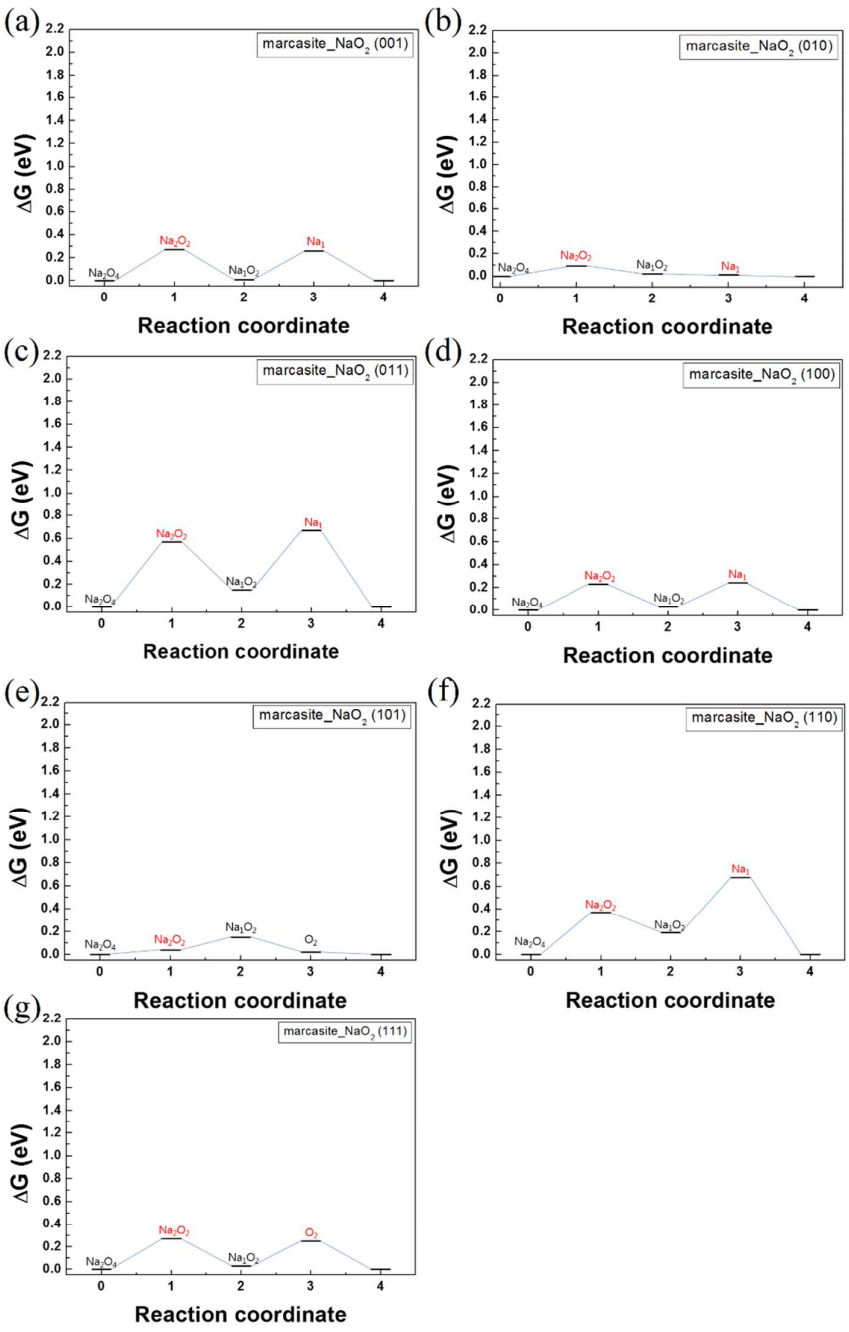

Figure S7. The OER energy profile for marcasite NaO_2. (a) (001) surface of marcasite NaO_2, (b) (010) surface of marcasite NaO_2, (c) (011) surface of marcasite NaO_2, (d) (100) surface of marcasite NaO_2, (e) (101) surface of marcasite NaO_2, (f) (110) surface of marcasite NaO_2, and (g) (111) surface of marcasite NaO_2. The most favorable reaction paths are shown. The chemical steps are shown in red.

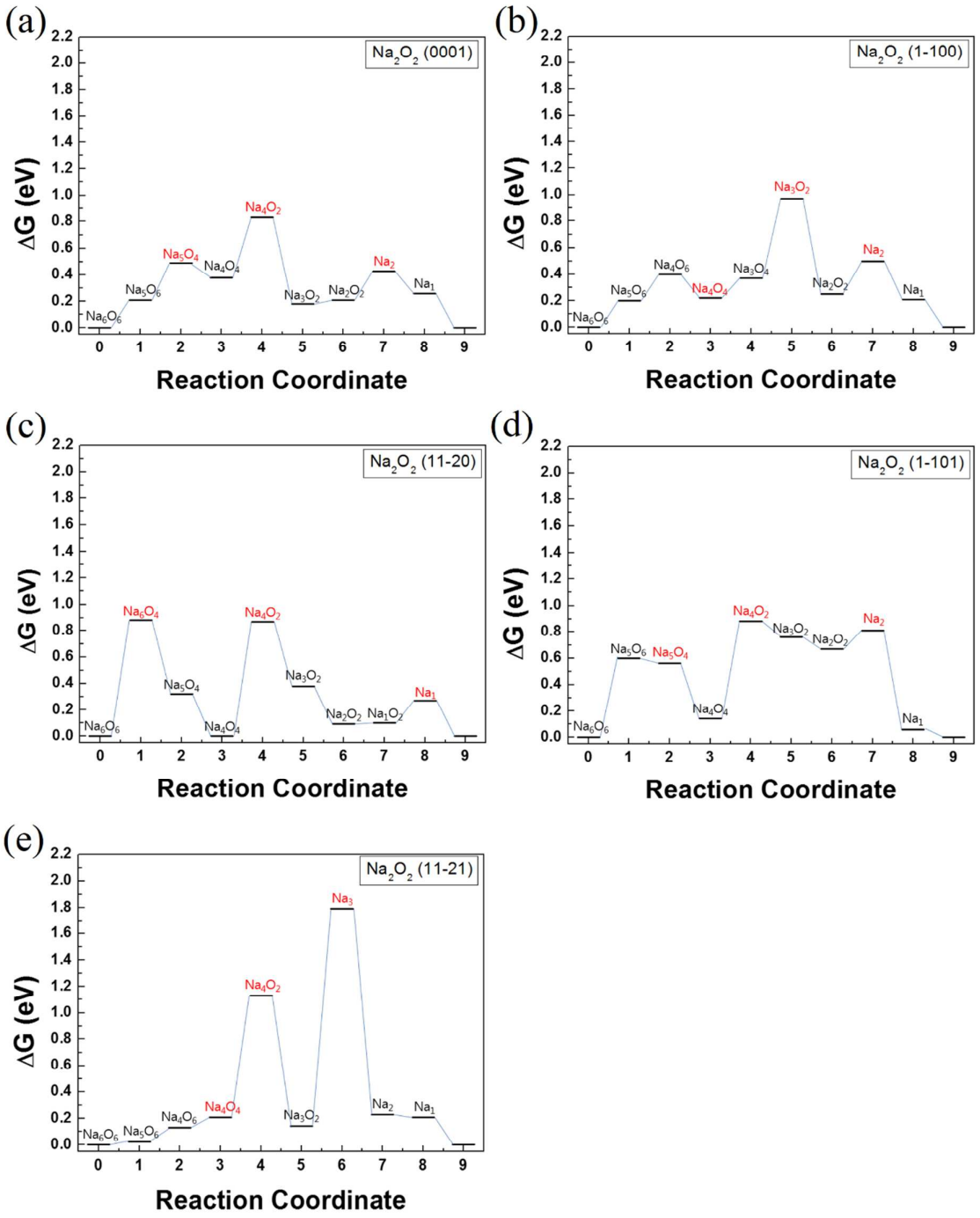

Figure S8. The OER energy profile for Na_2O_2. (a) The (0001) surface of Na_2O_2, (b) the $(1\bar{1}00)$ surface of Na_2O_2, (c) the $(11\bar{2}0)$ surface of Na_2O_2, (d) the $(1\bar{1}01)$ surface of Na_2O_2, and (e) the $(11\bar{2}1)$ surface of Na_2O_2. The most favorable reaction paths are shown. The chemical steps are shown in red.

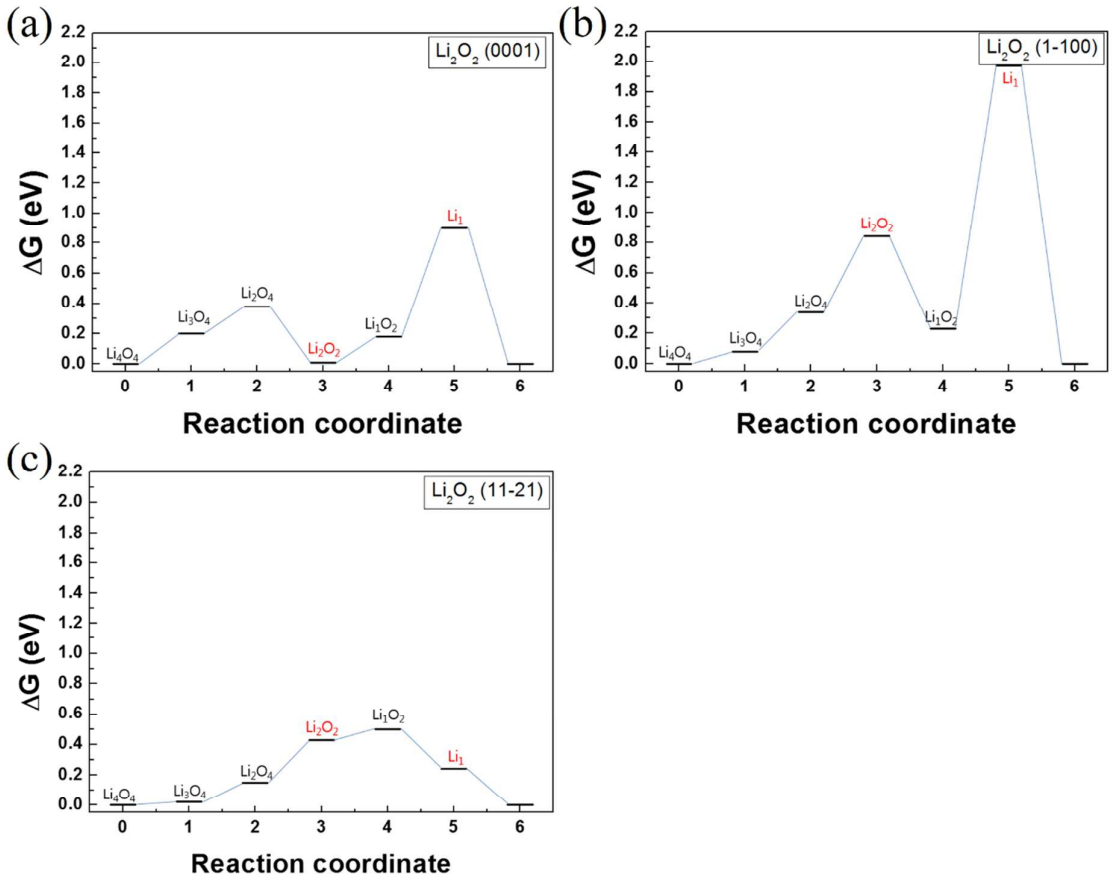

Figure S9. The OER energy profile for Li_2O_2. (a) (0001) surface of Li_2O_2, (b) $(1\bar{1}00)$ surface of Li_2O_2, and (c) $(11\bar{2}1)$ surface of Li_2O_2. The most favorable reaction paths are shown. The chemical steps are shown in red. Since $(11\bar{2}0)$ and $(1\bar{1}01)$ surfaces cannot be found in Wulff shape, the OER profiles of these surfaces were not calculated.

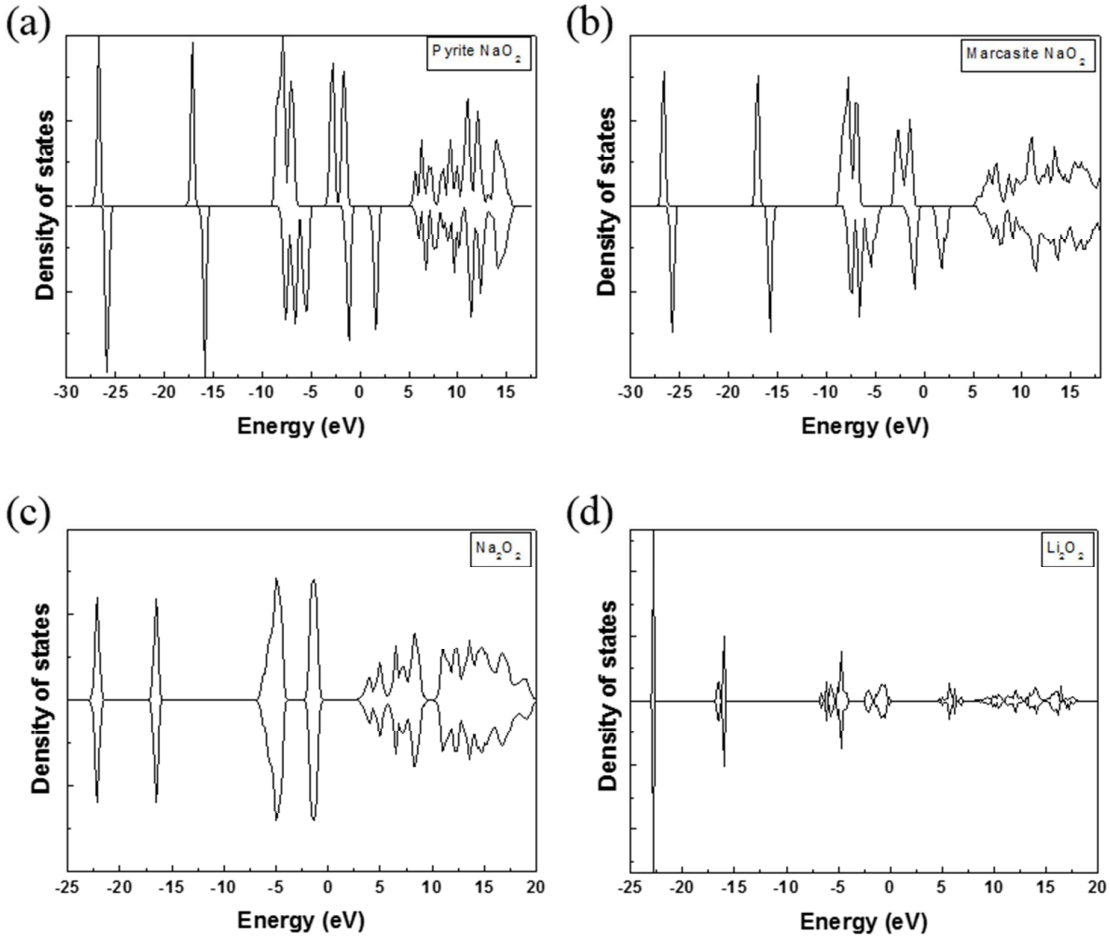

Figure S10. Density of state of (a) pyrite NaO_2, (b) marcasite NaO_2, (c) Na_2O_2, (d) Li_2O_2.